2024-02-29

Evaluation of modulus of elasticity of concrete containing both natural and recycled concrete aggregates

Li, Z

10.1016/j.jclepro.2024.141591
Journal of Cleaner Production
Elsevier BV

Journal of Cleaner Production xxx (xxxx) 141591

Contents lists available at ScienceDirect

Journal of Cleaner Production

journal homepage: www.elsevier.com/locate/jclepro

Evaluation of modulus of elasticity of concrete containing both natural and recycled concrete aggregates

Zaiwei Li [a], Long-yuan Li [b, *], Shanshan Cheng [b]

[a] School of Urban Railway Transportation, Shanghai University of Engineering Science, Shanghai, 201620, PR China
[b] School of Engineering, Computing and Mathematics, University of Plymouth, Plymouth, PL4 8AA, UK

ARTICLE INFO

Handling Editor: Jian Zuo

Keywords:
Recycled concrete aggregate
Concrete
Elastic modulus
Two-phase modelling
Effective medium approximation

ABSTRACT

There is growing requirement to use recycled aggregate in concrete to demote industrial wastes produced by construction sectors. Thus, to develop simple but meaningful formulations to assess the mechanical properties of concrete, when it is mixed with both natural and recycled aggregates, becomes essential. In the present study an analytical approach to calculate the elastic modulus of concrete containing both natural and recycled concrete aggregates is proposed. The approach is developed on the concept of effective medium approximation but considering the effect of Poisson's ratio. Two analytical formulas are derived. One is for the two-phase concrete (mortar and aggregate) that is mixed with 100% natural aggregate or 100% recycled concrete aggregate. The other is for the three-phase concrete (mortar, natural aggregate, and recycled concrete aggregate) that is mixed with both natural and recycled aggregates. The analytical formulations are validated using the results obtained from both the numerical simulations and experimental tests. The present analytical model not only provides the simple and meaningful formulations to calculate the effective elastic modulus but also can be used to directly examine the influence of mortar, natural aggregate, recycled concrete aggregate and its replacement ratio to natural aggregate on the elastic modulus of the mixed concrete.

1. Introduction

Social and economic development requires an increasing demand on infrastructure, particularly in developing countries. Concrete is one of the commonly used materials for infrastructure. In order to ensure sustainable and cost-effective but still profitable concrete production, the construction industry will have to develop alternative types of concrete that not only can improve energy efficiency but can also cut CO2 emissions and reduce the use of nature resources. Cutting down ordinary Portland cement content and replacing natural aggregate with recycled aggregate in concrete represents a novel technology, which engenders considerable interest in construction sector, particularly due to the growing emphasis on sustainability. Currently, recycled concrete aggregate (RCA) produced from demolition waste and/or crushed construction is the main type of the recycled aggregate used in concrete. The RCA generally consists of mortar and aggregate materials (e.g. slag, gravel and crushed stones) that are previously mixed in the concrete (Dhir and Lye, 2019). The concept of using RCA to substitute natural aggregate in concrete is not new. However, its practical implementation is not widely recognised. This is partly because the variability of the properties of RCA when it is taken directly from recycled concrete (Colangelo et al., 2021), and partly because the RCA might contain chlorides if the parent concrete has been served in marine environment.

To foster a wide utilization of recycled aggregate in concrete, numerous studies have been carried out by examining the mechanical and durability properties of the concrete in which natural aggregate is partially or fully substituted with RCA. For example, Xiao et al. (2005) presented an experimental investigation on the mechanical properties of the concrete mixed with five different replacement percentages of RCA to natural aggregate. Etxeberria et al. (2006) conducted the microstructure and material characterisation analyses of recycled aggregate concrete (RAC). Padmini et al. (2009) examined the effect of the grade of the recycled concrete on the mechanical properties of RAC. Cabral et al. (2010) investigated the mechanical properties of the concrete mixed by using different water-to-cement ratios and different substitution ratios of RCA to natural aggregate. Duan and Poon (2014) reported the mechanical properties of the concrete mixed with different amounts of old adhered mortar in RCAs. Pedro et al. (2014) examined the effect of RCAs obtained from different sources on the mechanical properties of the mixed concrete. Gholampour et al. (2017) proposed an analysis

* Corresponding author.
E-mail addresses: zaiweili@sues.edu.cn (Z. Li), long-yuan.li@plymouth.ac.uk (L.-y. Li), shanshan.cheng@plymouth.ac.uk (S. Cheng).

https://doi.org/10.1016/j.jclepro.2024.141591
Received 10 November 2023; Received in revised form 15 January 2024; Accepted 29 February 2024
0959-6526/

model for predicting the mechanical properties of RAC by using gene expression programming techniques. Shaikh (2017) examined the influence of silica fume on the early-age and long-term mechanical properties of RAC containing slag. Zhou and Chen (2017) presented an experimental study on the influence of the recycled crushed rock aggregate and recycled pebbles aggregate on the mechanical properties of RAC. Jayasuriya et al. (2018) examined the influence of adhered mortar content on the mechanical properties of RAC by using 2-D finite element analysis method. Gholampour and Ozbakkaloglu (2018) presented a study on the long-term properties of concretes mixed with RCA taken from parent concretes of different strengths. Bui et al. (2018) reported a study on RAC in which the RCA was improved by using sodium silicate and silica fume. Adessina et al. (2019) conducted the experimental and numerical investigations of RAC. Their work included the mechanical properties and chloride diffusion. Song et al. (2019) reported a study on the effects of the content and particle size of recycled glass on the damping ratio of RAC. Xu et al. (2020) reported an experimental study on the evaluation of using iron ore tailings to produce tailing RAC. Wang et al. (2020) presented an experimental study on the effect of specimen size on the compressive strength, splitting tensile strength, and elastic modulus of RAC. Khattab et al. (2021) examined the effect of elevated temperatures on the physical and mechanical properties of concrete with different water-to-cement ratios, made by replacing 20% of natural aggregate by recycled brick aggregate. Xu et al. (2021) reported the mechanical properties and resistance against the coupled deterioration of sulphate attack and freeze-thaw cycles of tailing RAC. Hu et al. (2021) investigated the mechanical properties, drying shrinkage, and nanoscale characteristics of the concrete prepared with zeolite powder precoated recycled aggregate. Zadeh et al. (2021) examined the carbonation treatment effect on the improvement of the mechanical and environmental properties of RCA. Tang et al. (2022) investigated the compressive and tensile strengths of RAC in which both the coarse and fine aggregates are substituted by RCA. Dang et al. (2022) examined the influences of pore structure and morphological characteristics of recycled fine aggregates from clay bricks on the mechanical properties of RAC. Wang et al. (2022) investigated the compressive strength, dynamic elastic modulus, and diffusivity of RAC with different RCA substitution ratios. Bai et al. (2022) reported an experimental study on the uniaxial compressive mechanical properties of RAC specimens with different silica fume contents at different strain rates. Htet et al. (2022) presented a work on the physical and mechanical properties of quaternary blended concrete with recycled coarse aggregates and crushed waste glass. Ye et al. (2022) investigated the mechanical properties of RAC mixed with different volume ratios of polypropylene fibre.

Recently, Zhao et al. (2023) examined the compressive strength, flexural strength, and elastic modulus of RAC in which the RCA was treated by using nano-SiO2. Aziez et al. (2023) investigated the mechanical properties of ordinary Portland cement concrete mixed with coarse recycled asphalt pavement aggregates. Zhang et al. (2023) presented a review article on carbonation mechanism related to CO2 mineralisation and hydration, microstructure and multiscale mechanical properties of concrete containing carbonated RCA. Huang et al. (2023) presented a comparison study on the mechanical properties of RAC between using RCA and recycled brick aggregate. Guo et al. (2023) presented an experimental investigation on the effects of lateral confining pressure and recycling cycles on the mechanical properties of RAC subjected to triaxial compression in which the concrete was mixed with the RCA that had been recycled several times. Note that apart from the use in ordinary Portland cement concrete, the RCA has been also used in geopolymer concrete (GPC). For instance, Shaikh (2016) investigated the mechanical and durability properties of fly ash-based GPC containing RCA. Damrongwiriyanupap et al. (2022) presented an assessment of mechanical properties of alkali-activated concrete containing RCA. Xie et al. (2019) examined the effect of combined usage of ground granulated blast-furnace slag and fly ash on the workability and mechanical properties of GPC mixed with RCA. Mesgari et al. (2020) presented a study on the recycling of GPC and the use of coarse recycled GPC aggregate in both the GPC and OPC concretes.

The above literature review shows that there are numerous research works on the mechanical properties of the concrete when it is mixed with different types of recycled aggregates. However, most of these works are the experimental studies, numerical analyses, and/or the applications of RCA in different types of concrete (Lin et al., 2023; Chen et al., 2023; Xu et al., 2022; Deresa et al., 2021). There are very few work on the analytical study. The modulus of elasticity of a material is one of the most important properties of the material because it represents the capacity of the material to resist deformation under an applied load. In this paper, an analytical approach is developed for the calculation of the elastic modulus of RAC when its aggregate involves both the natural and recycled aggregates. To demonstrate the reliability and rationality of the present model, the analytical formulations derived from the present model are validated using the results obtained from both the numerical simulations and experimental tests.

2. Two-phase spherical model for evaluating elastic modulus of concrete

Concrete is a composite material, which is composed of a large number of randomly distributed aggregates embedded in a hard matrix of cementitious material that fills the space between the aggregate particles and glues them together. The mechanical properties of the concrete thus are dependent on the properties and volume fractions of the matrix and aggregate.

Consider a two-phase, three-dimensional spherical model of concrete as shown in Fig. 1a, in which its outer layer represents the matrix and inner core represents the aggregate. Assume the sphere is subjected to a uniform radial tensile stress on its outer surface. According to the theory of elasticity (Timoshenko and Goodier, 1970) (page 453), the radial displacement and radial stress component in the aggregate and matrix can be expressed as follows.

In the aggregate where $0 \le r \le a$,

$$u^a(r) = C_1 r \tag{1}$$

$$\sigma_r^a(r) = \frac{E_1 C_1}{1 - 2\nu_1} \tag{2}$$

In the matrix where $a \le r \le b$,

$$u^m(r) = C_2 r + \frac{C_3}{r^2} \tag{3}$$

$$\sigma_r^m(r) = \frac{E_2 C_2}{1 - 2\nu_2} - \frac{2E_2 C_3}{1 + \nu_2}\frac{1}{r^3} \tag{4}$$

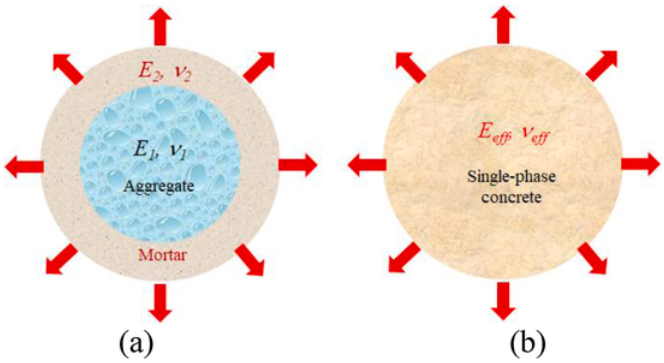

Fig. 1. (a) Two-phase spherical concrete model. (b) Single-phase spherical concrete model with effective properties.

where a and b are the inner and outer radius of the matrix, u and σ_r are the radial displacement and radial stress component, the superscript "a" and "m" represent the aggregate and matrix, respectively, r is the radial coordinate, E_1 and E_2 are the elastic moduli of the aggregate and matrix, ν_1 and ν_2 are the Poisson's ratios of the aggregate and matrix, respectively, C_1, C_2 and C_3 are the constants to be determined based on the stress boundary condition at outer surface, and the continuity conditions of radial displacement and radial stress component at the interface between the aggregate and matrix as follows,

$$\sigma_r^m(b) = \sigma_b \tag{5}$$
$$u^a(a) = u^m(a) \tag{6}$$
$$\sigma_r^a(a) = \sigma_r^m(a) \tag{7}$$

where σ_b is the radial tensile stress applied on the outer surface of the sphere. Substituting Eq. (4) into (5), Eqs. (1) and (3) into (6), and Eqs. (2) and (4) into (7), it yields,

$$\frac{E_2C_2}{1-2\nu_2} - \frac{2E_2C_3}{1+\nu_2}\frac{1}{b^3} = \sigma_b \tag{8}$$
$$C_1a = C_2a + \frac{C_3}{a^2} \tag{9}$$
$$\frac{E_1C_1}{1-2\nu_1} = \frac{E_2C_2}{1-2\nu_2} - \frac{2E_2C_3}{1+\nu_2}\frac{1}{a^3} \tag{10}$$

Solving Eqs. (8)–(10) for C_1, C_2 and C_3, it yields,

$$C_1 = C_2 + \frac{C_3}{a^3} = \frac{k_v\sigma_b}{\left(1+k_vV_a\right)E_1^* + k_v\left(1-V_a\right)E_2^*} \tag{11}$$
$$C_2 = \frac{\sigma_b}{E_2^*}\left(\frac{E_1^* + k_vE_2^*}{\left(1+k_vV_a\right)E_1^* + k_v\left(1-V_a\right)E_2^*}\right) \tag{12}$$
$$\frac{C_3}{a^3} = -\frac{\sigma_b}{E_2^*}\left(\frac{E_1^* - E_2^*}{\left(1+k_vV_a\right)E_1^* + k_v\left(1-V_a\right)E_2^*}\right) \tag{13}$$

where $k_v = \frac{2(1-2\nu_2)}{1+\nu_2}$, $E_1^* = \frac{E_1}{1-2\nu_1}$, $E_2^* = \frac{E_2}{1-2\nu_2}$, and $V_a = \frac{a^3}{b^3}$ is the volume fraction of aggregate in the mixture. The radial displacement of the outer surface of the sphere thus is given by,

$$u^m(b) = \frac{b\sigma_b}{E_2^*}\left(\frac{\left(1-V_a\right)E_1^* + \left(k_v+V_a\right)E_2^*}{\left(1+k_vV_a\right)E_1^* + k_v\left(1-V_a\right)E_2^*}\right) \tag{14}$$

If we treat the sphere as a single material by using the effective elastic modulus E_{eff} and effective Poisson's ratio ν_{eff}, as shown in Fig. 1b, then, according to Eqs. (1) and (2), the radial displacement of the outer surface of the sphere can be expressed as follows,

$$u(b) = \frac{b\sigma_b}{E_{eff}^*} \tag{15}$$

where $E_{eff}^* = \frac{E_{eff}}{1-2\nu_{eff}}$. The comparison of Eqs. (14) and (15) indicates that, if these two spheres have the same radial displacement on the outer surface when they are subjected to the same radial tensile stress on the outer surface, then the following equation must hold,

$$E_{eff}^* = \frac{\left(1+k_vV_a\right)E_1^* + k_v\left(1-V_a\right)E_2^*}{\left(1-V_a\right)E_1^* + \left(k_v+V_a\right)E_2^*}E_2^* \tag{16}$$

Eq. (16) can be used to calculate the effective elastic modulus of concrete containing mortar and aggregate. Interestingly, if $k_v = 2$ then Eq. (16) turns to the well-known expression given in the Maxwell model, which has been widely used for the prediction of electrical conductivity and thermal conductivity in two-phase composite materials and chloride diffusion coefficient in concrete materials (Fang et al., 2020, 2021a, 2021b, 2021c; Yuan et al., 2023; Li and Li, 2022). If, as an approximation, we take $\nu_2 = 1/5$ for the Poisson's ratio of the mortar, this gives $k_v = 1$. This indicates that Eq. (16) is slightly different from the Maxwell model. This is because the derivation of Eq. (16) considers the effect of Poisson's ratio, whereas in the Maxwell model, the effect of Poisson's ratio was ignored.

To explain the difference between the present model and other models reported in literature, Fig. 2 shows a comprehensive comparison between six different models for a two-phase concrete, in which the formulas used for parallel, series, Counto-I, and Counto-II models can be found in ref. (Zhou et al., 1995). In the present model the effective Poisson's ratio is assumed to be $\nu_{eff} = V_a\nu_1 + (1\text{-}V_a)\nu_2$, whereas for the Maxwell model all Poisson's ratios are assumed to be zero when Eq. (16) is used. The values used in the calculation for the elastic moduli and Poisson's ratios are $E_1 = 54$ GPa and $\nu_1 = 0.23$ for coarse aggregate (gravel), and $E_2 = 25$ GPa and $\nu_2 = 0.21$ for mortar. It can be observed from Fig. 2 that the parallel model provides the upper bound, whereas the series model gives the lower bound. Note that the parallel and series models have been widely used in fibre-reinforced composite materials for estimating the Young's modulus of composite materials. However, the accuracy of these two models is largely dependent on the volume fraction of the fibres used in the composite. In general, it is more appropriate to use the series model if the volume fraction of fibres is very small; whereas the parallel model should be used if the volume fraction of fibres is high. For concrete the volume fraction of aggregate is normally not over 0.6. Thus, neither the parallel model nor the series model would be accurate. In the Counto models the aggregate is assumed to be as a small square covered by the matrix in a large square. The difference between the two Counto models is only the four "corner" parts, which are treated as "in-series first followed by in-parallel" or "in-parallel first followed by in-series". This explains why the predicted values by them do not have significant difference. In the Maxwell model the aggregate is assumed to be a small sphere covered by the matrix in a large sphere. The Maxwell model is close to Counto-I model when the volume fraction of aggregate is very small. When the volume fraction becomes large the Maxwell model gives an overprediction. In contrast, the present model is between the two Counto models. The elastic modulus predicted by the present model is consistently lower than that predicted by the Maxwell model, indicating that the Poisson's ratio does have some effect on the effective elastic modulus.

Fig. 3 illustrates the variation of effective elastic modulus with the volume fraction of aggregate for three different types of aggregate. As it is expected, the effective elastic modulus increases with increased volume fraction of aggregate because the elastic modulus of the aggregate

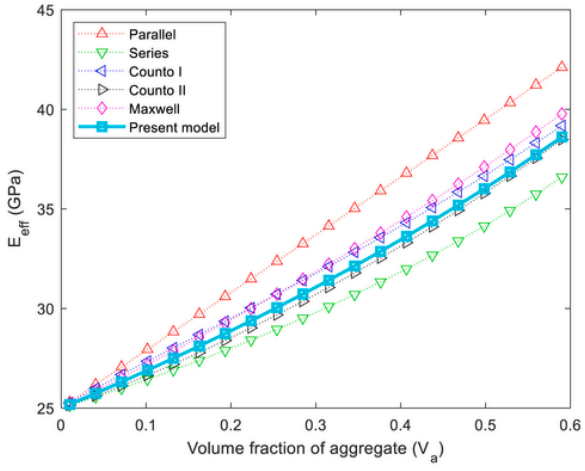

Fig. 2. Comparison of elastic moduli calculated using different approaches ($E_1 = 54$ GPa, $\nu_1 = 0.23$, $E_2 = 25$ GPa, $\nu_2 = 0.21$).

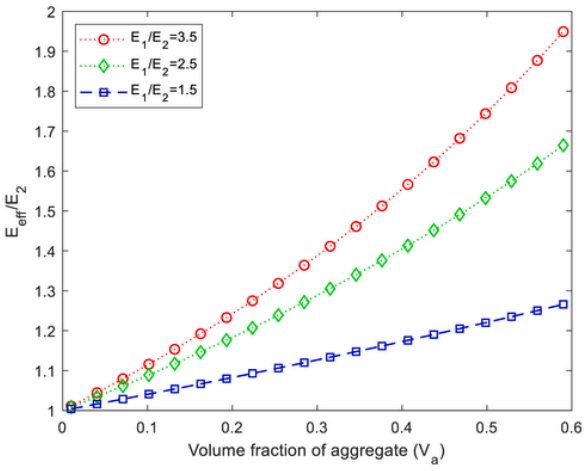

Fig. 3. Variation of effective elastic modulus with volume fraction of aggregate ($\nu_1 = 0.23$, $E_2 = 25$ GPa, $\nu_2 = 0.21$).

is generally larger than the elastic modulus of the mortar. The larger the elastic modulus of the aggregate, the quicker the increase of the effective elastic modulus of the concrete. For instance, the effective elastic modulus can be increased by 22%, 53% and 74%, respectively, when 50% volume fraction aggregate with elastic modulus $1.5E_2$, $2.5E_2$, and $3.5E_2$ is used.

Table 1 shows the comparison of the elastic moduli and Poisson's ratios between the present model and those obtained from the experiments for the concrete mixed using different types of coarse aggregate (expanded clay, sintered fly ash, limestone, gravel, glass, and steel). The experimental data were reported by Zhou et al. (1995) for the concretes at the age of 28 days, whereas the model prediction value is calculated using Eq. (16). It can be seen from the table that the elastic modulus and Poisson's ratio predicted from the present model are reasonably close to those measured in the experiments. This demonstrate that the elastic modulus of concrete can be evaluated based on the properties of mortar and aggregate mixed in the concrete by using the present two-phase model represented by Eq. (16).

3. Effective elastic modulus of concrete with both natural and recycled aggregates

It has been reported in literature (Dhir and Lye, 2019) that the elastic modulus of concrete will reduce when its mixture includes coarse RCA. The level of reduction is dependent on the mechanical properties of RCA, the content of RCA used in the mixture, and the mix design parameters of the concrete. The reason for this is because the RCA not only has adhered old mortar which is relatively softer than the aggregate itself but also could have mechanical damage during its recycling process (Yuan et al., 2023; Hu et al., 2018). To identify the influence mechanism of the replacement ratio of RCA to natural aggregate on the elastic modulus of the mixed concrete, the effective medium approximation (EMA) is used and modified herein. Note that the original version of EMA was developed to describe the macroscopic properties of two-phase materials (Bruggeman, 1935; Landauer, 1952). When it is used for calculating the effective elastic modulus of two-phase materials, the EMA can be written as follows,

$$\frac{E_{eff}-E_1}{2E_{eff}+E_1}V_1+\frac{E_{eff}-E_2}{2E_{eff}+E_2}V_2=0 \tag{17}$$

where E_1 and V_1 are the elastic modulus and volume fraction of the material in phase 1, E_2 and V_2 are the elastic modulus and volume fraction of the material in phase 2, and $V_1+V_2\equiv 1$. Eq. (17) can be rewritten as follows,

$$\frac{V_1}{\frac{1}{3}E_1+\frac{2}{3}E_{eff}}+\frac{V_2}{\frac{1}{3}E_2+\frac{2}{3}E_{eff}}=\frac{1}{E_{eff}} \tag{18}$$

Note that Eq. (18) cannot be directly applied to the concrete that contains both natural and recycled aggregates because apart from natural and recycled aggregates, there is a mortar phase in the concrete. However, if the concrete is treated as a random mixture of concrete 1, which is made of mortar and natural aggregate alone, and concrete 2, which is made of mortar and RCA alone, then Eq. (18) can be expressed as follows,

$$\frac{1-x}{\frac{1}{3}E_o+\frac{2}{3}E_{eff}}+\frac{x}{\frac{1}{3}E_{100}+\frac{2}{3}E_{eff}}=\frac{1}{E_{eff}} \tag{19}$$

where x is the substitution ratio of RCA to natural aggregate, E_o and E_{100} are the elastic moduli of the concrete 1 with 0% RCA (100% natural aggregate) and concrete 2 with 100% RCA (0% natural aggregate), respectively. For a given concrete, E_o and E_{100} can be calculated directly using Eq. (16) in terms of the elastic moduli and Poisson's ratios of the mortar, natural aggregate and RCA. It is obvious that concrete 1 and concrete 2 are mathematically symmetric in Eq. (19), which implies that the natural aggregate and RCA are independent in the mixture. Fig. 4 provides a graphical interpretation of Eq. (19) when it is applied to the three-phase concrete with mortar, natural aggregate and RCA.

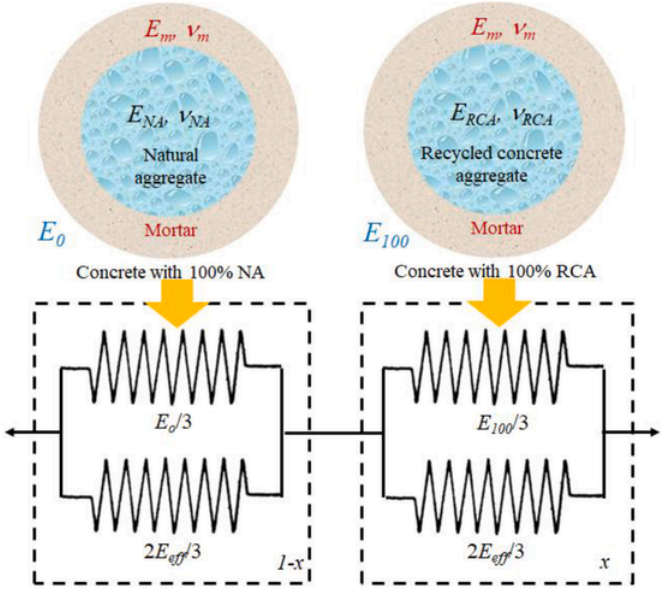

Fig. 4. Spring model interpretation of effective medium approximation.

Table 1
Comparison of elastic moduli obtained from model prediction and test for concrete with aggregate volume fraction $V_a = 0.425$.

Component	Elastic modulus (GPa)	Poisson's ratio	E_{eff} (GPa) (Test) (Zhou et al., 1995)	E_{eff} (GPa) (Model)	ν_{eff} (Test)	ν_{eff} (Model)
Mortar (matrix)	40.8	0.21	–	–	–	–
Expanded clay	5.2	0.41	18.6	20.1	0.29	0.295
Sintered fly ash	18.2	0.28	30.2	29.3	0.26	0.240
Limestone	56	0.29	49.5	46.9	0.27	0.244
Gravel	54	0.23	51.3	45.9	0.21	0.219
Glass	72	0.26	52.8	51.5	0.25	0.231
Steel	210	0.30	69.9	69.0	0.28	0.248

By rearranging Eq. (19), the effective elastic modulus of concrete mixed with both natural aggregate and RCA can be expressed as follows,

$$E_{eff} = \frac{-(1-3x)E_{100} - (3x-2)E_o + \sqrt{[(1-3x)E_{100} + (3x-2)E_o]^2}}{4}$$

It is obvious from Eq. (20) that, if $x = 0$ then $E_{eff} = E_o$ and if $x = 1$ then $E_{eff} = E_{100}$. Eq. (20) shows that E_{eff} is a nonlinear function of x, E_0 and E_{100}, and as x increases from 0 to 1, E_{eff} varies from E_0 to E_{100}. Eq (20) together with Eq. (16) can be used to calculate the effective elastic modulus of concrete mixed with both natural aggregate and RCA. The input parameters required for the calculation of E_{eff} are the elastic moduli and Poison's ratios of the mortar, natural aggregate and RCA, the volume fraction of mortar, and the replacement ratio of RCA to natural aggregate used in the concrete mix. These parameters can be easily obtained from the tests of individual materials (mortar, natural aggregate, and RCA) and the mixing design parameters (volume fraction of mortar and the replacement ratio of RCA to natural aggregate) used for the concrete mixture.

Fig. 5 graphically illustrate the effect of the elastic modulus of RCA on the relative value of the effective elastic modulus of the concretes mixed with three different types of RCA calculated using Eq. (20), in which E_o and E_{100} are calculated using Eq. (16). The elastic moduli and Poisson's ratios of individual components used in the calculation are $E_m = 18$ GPa, $\nu_m = 0.25$, $E_{NA} = 54$ GPa, $\nu_{NA} = 0.25$, and $\nu_{RCA} = 0.24$. The volume fraction of natural aggregate plus RCA is $V_a = 0.52$. It is observed from Fig. 5 that the relative modulus reduces with increased replacement ratio of RCA to natural aggregate. The reduction seems quicker for the concrete with lower elastic modulus RCA. For example, the relative modulus of the concrete with 100% replacement of RCA with elastic modulus $E_{RCA} = 0.4E_{NA}$, $E_{RCA} = 0.6E_{NA}$ and $E_{RCA} = 0.8E_{NA}$ is about 0.65, 0.80 and 0.90, respectively.

Fig. 6 displays the effect of the elastic modulus of mortar on the relative value of the effective elastic modulus of the concrete, in which the elastic moduli and Poisson's ratios of individual components used in the calculation are $E_{NA} = 54$ GPa, $\nu_{NA} = 0.25$, $E_{RCA} = 30$ GPa, $\nu_{RCA} = 0.24$, and $\nu_m = 0.25$. Again, the volume fraction of natural aggregate plus RCA is $V_a = 0.52$. It can be seen from Fig. 6 that, when the effective elastic modulus is normalised by using the elastic modulus of the concrete mixed with 100% natural aggregate, the difference between the variation curves with different mortars seems not substantial, particularly when the mortar has higher elastic modulus value. For example, the relative modulus of the concrete with 100% replacement of RCA with elastic modulus $E_m = 0.3E_{NA}$, $E_m = 0.5E_{NA}$ and $E_m = 0.7E_{NA}$ is about 0.77, 0.75 and 0.74, respectively.

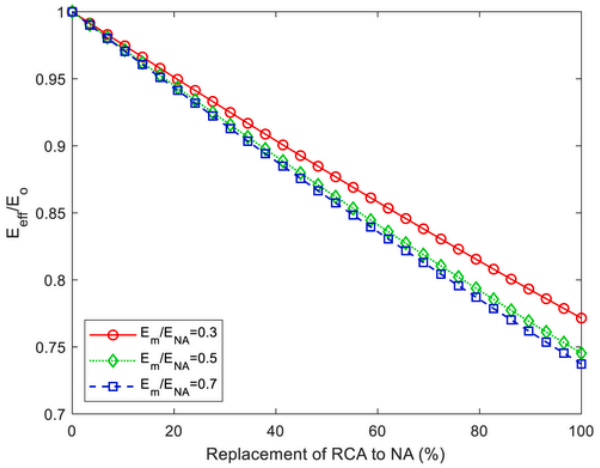

Fig. 6. Effect of elastic modulus of mortar on effective elastic modulus ($V_a = 0.52$, $\nu_m = 0.25$, $E_{NA} = 54$ GPa, $\nu_{NA} = 0.25$, $E_{RCA} = 30$ GPa, $\nu_{RCA} = 0.24$).

To validate the present three-phase model described by Eq. (20), experimental data obtained from Zheng et al. (2023) and Liu et al. (2023) are utilized. Fig. 7 shows the comparison of the present model prediction using Eq. (20) with Zheng et al. experimental data (Zheng et al., 2023). In Zheng et al. experiment, the natural aggregate was gravel, and the RCA was recycled brick aggregate. The geopolymer concrete (GPC) and ordinary Portland cement (OPC) concrete were mixed by using five different substitution ratios of RCA to natural aggregate. In the calculation, the elastic moduli of concretes with 0% RCA and 100% RCA are $E_o = 21.5$ GPa and $E_{100} = 10$ GPa for GPC, and $E_o = 32.5$ GPa and $E_{100} = 19$ GPa for OPC concrete, respectively. Fig. 8 shows the comparison of the present model prediction using Eq. (20) with Liu et al. experimental data (Liu et al., 2023). In Liu et al. experiment, the natural aggregate was crushed stone, and the RCA was obtained from concrete beams and columns in a demolished house. Two

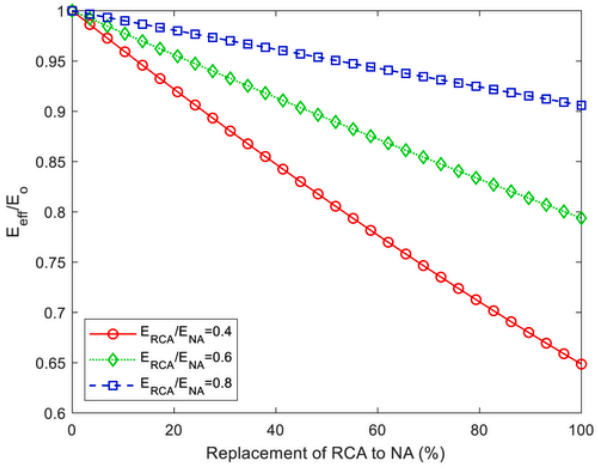

Fig. 5. Effect of elastic modulus of RCA on effective elastic modulus ($V_a = 0.52$, $E_m = 18$ GPa, $\nu_m = 0.25$, $E_{NA} = 54$ GPa, $\nu_{NA} = 0.25$, $\nu_{RCA} = 0.24$).

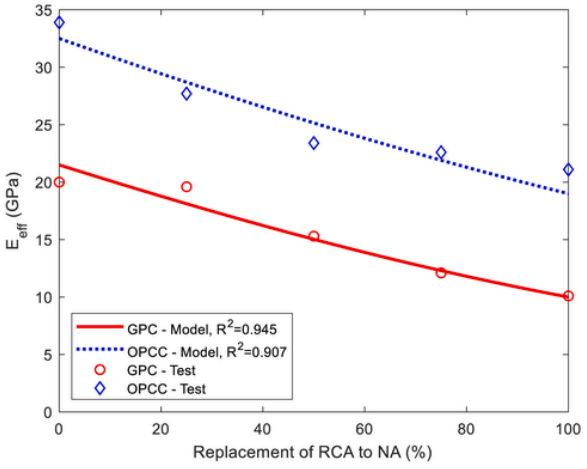

Fig. 7. Comparison between model prediction and experimental data (Zheng et al., 2023)
(GPC: $E_o = 21.5$ GPa, $E_{100} = 10$ GPa; OPC concrete: $E_o = 32.5$ GPa, $E_{100} = 19$ GPa).

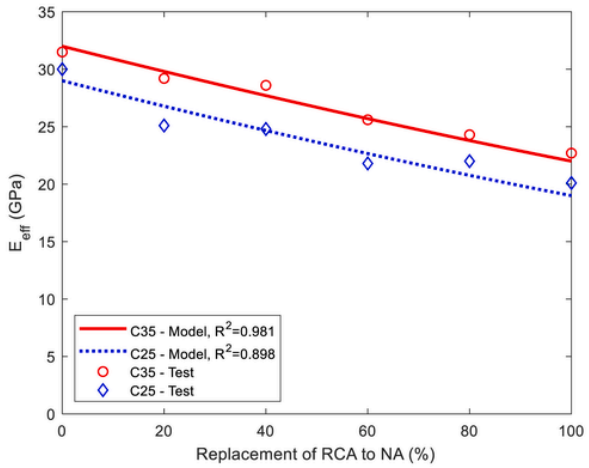

Fig. 8. Comparison between model prediction and experimental data (Liu et al., 2023)
(C35: E_o = 32 GPa, E_{100} = 22 GPa; C25: E_o = 29 GPa, E_{100} = 19 GPa).

concrete mixes with target strength for C25 and C35 were mixed by using six different substitution ratios of RCA to natural aggregate. In the calculation, the elastic moduli of concretes with 0% RCA and 100% RCA are E_o = 32 GPa and E_{100} = 22 GPa for C35, and E_o = 29 GPa and E_{100} = 19 GPa for C25, respectively. It can be observed from Figs. 7 and 8 that the effective elastic modulus predicted using the present model agrees generally well with that measured in experiments. This demonstrates that the three-phase model developed by modifying EMA to calculate the effective elastic modulus of the concrete mixed with both natural and recycled concrete aggregates is logical and reliable.

To further demonstrate the modified EMA model in which the predicted elastic modulus is calculated using Eq. (20) based on the experimentally obtained E_o and E_{100} values, Fig. 9 plots a comparison between the effective elastic modulus calculated using Eq. (20) and that measured in experiments, taken from López-Gayarre et al. (2011) and Yang et al. (2008) for concretes with different replacement ratios of RCA to natural aggregate. It can be seen from the figure that there is a good agreement between the predictions and experiments.

The above validation of Eq. (20) is based on the known elastic modulus values of concrete with 0% and 100% RCA. If the concrete is represented by mortar, natural aggregate, and RCA, then Eqs. (16) and (20) need be used together to calculate the effective elastic modulus of the concrete. To demonstrate the reliability of the present approach, a two-dimensional plane stress linear finite element analysis (FEA) model, as shown in Fig. 10a,is developed, in which the geometry represents one quarter of a concrete block. In the stress analysis the horizontal displacement of the line OA and the vertical displacement of the line OC (see Fig. 10a) are restrained. The line AB is the displacement control boundary and has a negative vertical displacement of 0.001 m. The line BC has a free boundary condition. The dimensions of the geometry are 0.05 m (width) and 0.10 m (length). The volume fraction of mortar is assumed to be V_m = 0.48. The volume fractions of natural aggregate and RCA vary with the replacement percentage of RCA to natural aggregate, but the sum of them remains to be 0.52. The elastic moduli and Poisson's ratios of the mortar, natural aggregate, and RCA used in the simulation are given in Table 2. The effective elastic modulus of the concrete is calculated based on the average compressive stress on the boundary OC and the average compressive strain applied (1%). Both the natural aggregate and RCA are modelled as randomly distributed circles. Due to the small size of aggregates an adaptive mesh scheme was used in the analysis to ensure the accuracy of the results obtained (Li et al., 1995, 2012). Fig. 10b shows the finite element mesh employed in the analysis. The analysis is carried out by using commercial software COMSOL. Fig. 11 shows the comparison of the effective elastic modulus values obtained from the FEA and that calculated using Eqs. (16) and (20) for two different cases as shown in Table 2. It can be seen from Fig. 11 that the effective modulus calculated from Eqs. (16) and (20) is very close to that obtained from the FEA. This demonstrate that the three-phase model developed herein can provide good prediction of the effective elastic modulus of the concrete containing both natural and recycled concrete aggregates. Compared to the FEA, the present analytical approach is much simple and convenient to use. It also has clear physical meaning.

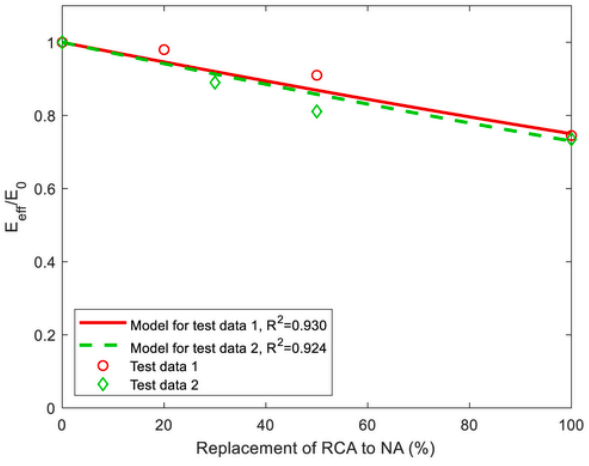

Fig. 9. Comparison between model prediction and experimental data
(Test data 1 and 2 are taken from Refs. (Liu et al., 2023; Yang et al., 2008), respectively).

4. Conclusions

An analytical model has been reported in the present paper for calculating the effective elastic modulus of concrete containing both natural and recycled concrete aggregates. Two analytical formulas have been derived. One is for the two-phase concrete that is mixed with 100% natural aggregate or 100% RCA. The other is for the three-phase concrete that is mixed with both natural and recycled concrete aggregates. The rationality and correctness of the present model have been demonstrated by using both the test data published in literature and the numerical results obtained from our own finite element analysis. From the results obtained, the following conclusions can be drawn.

- The present two-phase model described by Eq. (16) takes into account the effect of Poisson's ratio, which appears important when the mortar, natural aggregate, and RCA have distinct Poisson's ratios. The effective elastic modulus when the Poisson's ratio effect is considered will be lower than that calculated using Maxwell model.
- The present three-phase model described by Eqs. (16) and (20) is simple, meaningful, and convenient to use. The model has a symmetric feature for the natural and recycled concrete aggregates mixed in concrete. The model reflects a direct effect of the use of RCA on the elastic modulus of the mixed concrete.
- The effective elastic modulus of concrete is dependent on both the modulus ratio and substitution ratio of RCA to natural aggregate. It decreases with the increase of substitution ratio of RCA to natural aggregate, but increases with the increased modulus ratio of RCA to natural aggregate.
- The effective elastic modulus of concrete is also influenced by the modulus ratio of mortar to RCA. However, when the effective

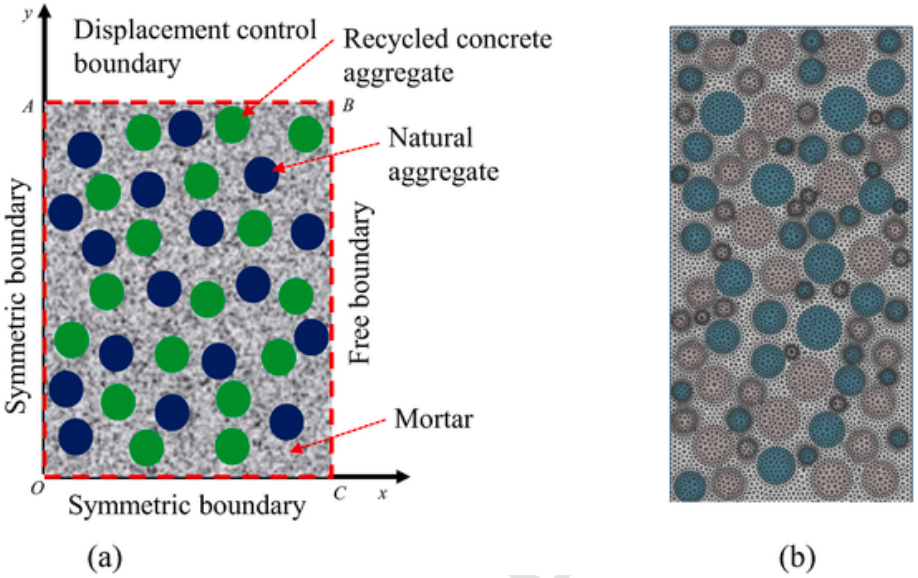

Fig. 10. (a) Schematic of finite element analysis model of three-phase concrete containing mortar, natural aggregate and recycled concrete aggregate. (b) Finite element mesh.

Table 2
Elastic modulus and Poison's ratio of components used in concrete.

Component	Mortar		Natural aggregate		Recycled concrete aggregate	
	E_1 (GPa)	ν_1	E_2 (GPa)	ν_2	E_3 (GPa)	ν_3
Case 1	18	0.25	54	0.23	35	0.24
Case 2	18	0.25	54	0.23	25	0.24

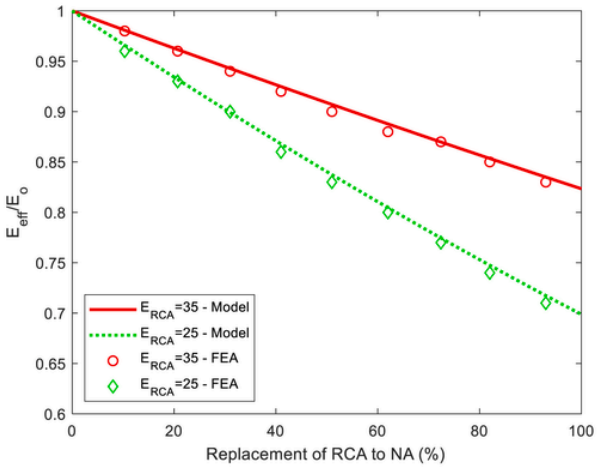

Fig. 11. Comparison between model prediction and FEA results.

elastic modulus is normalised by using the elastic modulus of the concrete mixed with 100% natural aggregate, its value is less sensitive to the change of mortar's elastic modulus.

CRediT authorship contribution statement

Zaiwei Li: Conceptualization, Formal analysis, Investigation, Methodology, Validation, Writing – review & editing. **Long-yuan Li:** Conceptualization, Formal analysis, Investigation, Methodology, Supervision, Validation, Writing – original draft, Writing – review & editing. **Shanshan Cheng:** Conceptualization, Formal analysis, Investigation, Methodology, Visualization, Writing – review & editing.

Declaration of competing interest

The authors declare that they have no known competing financial interests or personal relationships that could have appeared to influence the work reported in this paper.

Data availability

No data was used for the research described in the article.

Acknowledgements

The authors would like to acknowledge the financial support received from the National Natural Science Foundation of China (Grant No. 52178430), and the European Commission Research Executive Agency via a Marie Skłodowska-Curie Research and Innovation Staff Exchange project (H2020-MSCA-RISE-2017, TRAC-777823).

References

Adessina, A., Fraj, A.B., Barthélémy, J.F., Chateau, C., Garnier, D., 2019. Experimental and micromechanical investigation on the mechanical and durability properties of recycled aggregates concrete. Cement Concr. Res. 126, 105900.
Aziez, M.N., Achour, A., Bahaz, A., Lakhdari, Z., 2023. Effect of waste brick powder rich in SiO2 on the physical and mechanical properties of Portland cement concrete containing coarse recycled asphalt pavement aggregates (RAP). J. Build. Eng. 76, 107337.
Bai, W., Shen, J.X., Guan, J.F., Wang, J.Y., Yuan, C.Y., 2022. Study on compressive mechanical properties of recycled aggregate concrete with silica fume at different strain rates. Mater. Today Commun. 31, 103444.
Bruggeman, D.A.G., 1935. Berechnung verschiedener physikalischer Konstanten von heterogenen Substanzen. I. Dielektrizitätskonstanten und Leitfähigkeiten der Mischkörper aus isotropen Substanzen. Ann. Phys. 416 (7), 636–664.
Bui, N.K., Satomi, T., Takahashi, H., 2018. Mechanical properties of concrete containing 100% treated coarse recycled concrete aggregate. Construct. Build. Mater. 163, 496–507.
Cabral, A.E.B., Schalch, V., Molin, D.C.C.D., Ribeiro, J.L.D., 2010. Mechanical properties modeling of recycled aggregate concrete. Construct. Build. Mater. 24 (4), 421–430.
Chen, W.G., Xu, J.J., Li, Z.P., Huang, X.L., Wu, Y.T., 2023. Load-carrying capacity of circular recycled aggregate concrete-filled steel tubular stub columns under axial compression: reliability analysis and design factor calibration. J. Build. Eng. 66, 105935.
Colangelo, F., Petrillo, A., Farina, I., 2021. Comparative environmental evaluation of recycled aggregates from construction and demolition wastes in Italy. Sci. Total Environ. 798, 149250.
Damrongwiriyanupap, N., Srikhamma, T., Plongkrathok, C., Phoo-ngernkham, T., Sae-Long, W., Hanjitsuwan, S., Sukontasukkul, P., Li, L.Y., Chindaprasirt, P., 2022. Assessment of equivalent substrate stiffness and mechanical properties of sustainable

alkali-activated concrete containing recycled concrete aggregate. Case Stud. Constr. Mater. 16, e00982.
Dang, J.T., Xiao, J.Z., Duan, Z.H., 2022. Effect of pore structure and morphological characteristics of recycled fine aggregates from clay bricks on mechanical properties of concrete. Construct. Build. Mater. 358, 129455.
Deresa, S.T., Xu, J.J., Shan, B., Ren, H.T., Xiao, Y., 2021. Experimental investigation on flexural behavior of full-scale glued laminated bamboo (glubam)-concrete composite beams: a case study of using recycled concrete aggregates. Eng. Struct. 233, 111896.
Dhir, R.K., Lye, C.Q., 2019. Recycled Aggregates: Use in Concrete. Thomas Telford Limited, London.
Duan, Z.H., Poon, C.S., 2014. Properties of recycled aggregate concrete made with recycled aggregates with different amounts of old adhered mortars. Mater. Des. 58, 19–29.
Etxeberria, M., Vázquez, E., Mari, A., 2006. Microstructure analysis of hardened recycled aggregate concrete. Mag. Concr. Res. 58, 683–690.
Fang, Y., Li, L.Y., Jang, S.H., 2020. Calculation of electrical conductivity of self-sensing carbon nanotube composites. Compos. B Eng. 199, 108314.
Fang, Y., Hu, S.W., Li, L.Y., Jang, S.H., 2021a. Percolation threshold and effective properties of CNTs-reinforced two-phase composite materials. Mater. Today Commun. 29, 102977.
Fang, Y., Li, L.Y., Mawulé Dassekpo, J.B., Jang, S.H., 2021b. Heat transfer modelling of carbon nanotube reinforced composites. Compos. B Eng. 225, 109280.
Fang, Y., Li, L.Y., Jang, S.H., 2021c. Piezoresistive modelling of CNTs reinforced composites under mechanical loadings. Compos. Sci. Technol. 208, 108757.
Gholampour, A., Ozbakkaloglu, T., 2018. Time-dependent and long-term mechanical properties of concretes incorporating different grades of coarse recycled concrete aggregates. Eng. Struct. 157, 224–234.
Gholampour, A., Gandomi, A.H., Ozbakkaloglu, T., 2017. New formulations for mechanical properties of recycled aggregate concrete using gene expression programming. Construct. Build. Mater. 130, 122–145.
Guo, Y.P., Lei, B., Yu, L.J., Lin, X.Q., Li, W.G., 2023. Investigation on mechanical properties and failure criterion of multi-recycled aggregate concrete under triaxial compression. Procedia Struct. Integr. 45, 66–73.
Htet, P., Chen, W.S., Hao, H., Shaikh, F., 2022. Physical and mechanical properties of quaternary blended concrete with recycled coarse aggregates and crushed waste glass. Construct. Build. Mater. 353, 129016.
Hu, Z., Mao, L.X., Xia, J., Liu, J.B., Gao, J., Yang, J., Liu, Q.F., 2018. Five-phase modelling for effective diffusion coefficient of chlorides in recycled concrete. Mag. Concr. Res. 70 (11), 583–594.
Hu, H.B., He, Z.H., Shi, J.Y., Liang, C.F., Shibro, T.G., Liu, B.J., Yang, S.Y., 2021. Mechanical properties, drying shrinkage, and nano-scale characteristics of concrete prepared with zeolite powder pre-coated recycled aggregate. J. Clean. Prod. 319, 128710.
Huang, W., Quan, W.L., Miao, X.W., An, Y.J.N., Sun, W.B., 2023. Study on the compressive mechanical properties of mixed recycled aggregate concrete with silane modified. J. Build. Eng. 75, 106950.
Jayasuriya, A., Adams, M.P., Bandelt, M.J., 2018. Understanding variability in recycled aggregate concrete mechanical properties through numerical simulation and statistical evaluation. Construct. Build. Mater. 178, 301–312.
Khattab, M., Hachemi, S., Al Ajlouni, M.F., 2021. Evaluating the physical and mechanical properties of concrete prepared with recycled refractory brick aggregates after elevated temperatures' exposure. Construct. Build. Mater. 311, 125351.
Landauer, R., 1952. The electrical resistance of binary metallic mixtures. J. Appl. Phys. 23 (7), 779–784.
Li, Z.W., Li, L.Y., 2022. Analysis of electrical conductivity of carbon nanotube-reinforced two-phase composites. Compos. Commun. 35, 101305.
Li, L.Y., Bettess, P., Bull, J., Bond, T., Applegarth, I., 1995. Theoretical formulations for adaptive finite element computations. Commun. Numer. Methods Eng. 11 (10), 857–868.
Li, L.Y., Xia, J., Lin, S.S., 2012. A multi-phase model for predicting the effective diffusion coefficient of chlorides in concrete. Construct. Build. Mater. 26 (1), 295–301.
Lin, L., Xu, J.J., Yuan, J.L., Yu, Y., 2023. Compressive strength and elastic modulus of RBAC: an analysis of existing data and an artificial intelligence based prediction. Case Stud. Constr. Mater. 18, e02184.
Liu, B., Zhang, B., Wang, Z.Z., Bai, G.L., 2023. Study on the stress–strain full curve of recycled coarse aggregate concrete under uniaxial compression. Construct. Build. Mater. 363, 129884.
López-Gayarre, F., López-Colina, C., Serrano-López, M.A., García Taengua, E., López Martínez, A., 2011. Assessment of properties of recycled concrete by means of a highly fractioned factorial design of experiment. Construct. Build. Mater. 25 (10), 3802–3809.
Mesgari, S., Akbarnezhad, A., Xiao, J.Z., 2020. Recycled geopolymer aggregates as coarse aggregates for Portland cement concrete and geopolymer concrete: effects on mechanical properties. Construct. Build. Mater. 236, 117571.
Padmini, A., Ramamurthy, K., Mathews, M., 2009. Influence of parent concrete on the properties of recycled aggregate concrete. Construct. Build. Mater. 23, 829–836.
Pedro, D., De Brito, J., Evangelista, L., 2014. Influence of the use of recycled concrete aggregates from different sources on structural concrete. Construct. Build. Mater. 71, 141–151.
Shaikh, F.U.A., 2016. Mechanical and durability properties of fly ash geopolymer concrete containing recycled coarse aggregates. Int. J. Sustain. Built Environ. 5 (2), 277–287.
Shaikh, F.U.A., 2017. Mechanical properties of recycled aggregate concrete containing ternary blended cementitious materials. Int. J. Sustain. Built Environ. 6 (2), 536–543.
Song, W., Zou, D.J., Liu, T.J., Teng, J., Li, L., 2019. Effects of recycled CRT glass fine aggregate size and content on mechanical and damping properties of concrete. Construct. Build. Mater. 202, 332–340.
Tang, Y.X., Xiao, J.Z., Zhang, H.H., Duan, Z.H., Xia, B., 2022. Mechanical properties and uniaxial compressive stress-strain behavior of fully recycled aggregate concrete. Construct. Build. Mater. 323, 126546.
Timoshenko, S.P., Goodier, J.N., 1970. Theory of Elasticity, third ed. McGraw-Hill Book Company, London.
Wang, W.J., Liu, Y.Z., Qin, X.C., Li, Z., Duan, P.F., Dong, X.Q., 2020. Size effects on mechanical properties of recycled aggregate thermal insulation concrete. Construct. Build. Mater. 264, 120179.
Wang, Y.Z., Liu, Z., Wang, Y.C., Li, Q.M., Gong, X.L., Zhao, Y.P., 2022. Effect of recycled aggregate and supplementary cementitious material on mechanical properties and chloride permeability of concrete. J. Clean. Prod. 369, 133322.
Xiao, J.Z., Li, J.B., Zhang, C., 2005. Mechanical properties of recycled aggregate concrete under uniaxial loading. Cement Concr. Res. 35 (6), 1187–1194.
Xie, J.H., Wang, J.J., Rao, R., Wang, C.H., Fang, C., 2019. Effects of combined usage of GGBS and fly ash on workability and mechanical properties of alkali activated geopolymer concrete with recycled aggregate. Compos. B Eng. 164, 179–190.
Xu, F., Wang, S.L., Li, T., Liu, B., Li, B.B., Zhou, Y., 2020. The mechanical properties of tailing recycled aggregate concrete and its resistance to the coupled deterioration of sulfate attack and wetting–drying cycles. Structures 27, 2208–2216.
Xu, F., Wang, S.L., Li, T., Liu, B., Zhao, N., Liu, K.N., 2021. The mechanical properties and resistance against the coupled deterioration of sulfate attack and freeze-thaw cycles of tailing recycled aggregate concrete. Construct. Build. Mater. 269, 121273.
Xu, J.J., Chen, W.G., Yu, Y., Xu, J.G., Zhao, X.Y., 2022. Data-driven analysis on compressive behavior of unconfined and confined recycled aggregate concretes. Construct. Build. Mater. 356, 129282.
Yang, K.H., Chung, H.S., Ashour, A.F., 2008. Influence of type and replacement level of recycled aggregates on concrete properties. ACI Mater. J. 105 (3), 289–296.
Ye, P.H., Chen, Z.P., Su, W.W., 2022. Mechanical properties of fully recycled coarse aggregate concrete with polypropylene fiber. Case Stud. Constr. Mater. 17, e01352.
Yuan, W.B., Mao, L., Li, L.Y., 2023. A two-step approach for calculating chloride diffusion coefficient in concrete with both natural and recycled concrete aggregates. Sci. Total Environ. 856 (Part 2), 159197.
Zadeh, A.H., Mamirov, M., Kim, S., Hu, J., 2021. CO2-treatment of recycled concrete aggregates to improve mechanical and environmental properties for unbound applications. Construct. Build. Mater. 275, 122180.
Zhang, T., Chen, M., Wang, Y.T., Zhang, M.Z., 2023. Roles of carbonated recycled fines and aggregates in hydration, microstructure and mechanical properties of concrete: a critical review. Cement Concr. Compos. 138, 104994.
Zhao, W., Liu, J.L., Guo, H.Y., Li, L.F., 2023. Effect of nano-SiO2 modified recycled coarse aggregate on the mechanical properties of recycled concrete. Construct. Build. Mater. 395, 132319.
Zheng, Y.Q., Zheng, L.Y., Wang, Y.Q., 2023. Compressive performance and stress–strain relationship of geopolymer recycled brick aggregate concrete. Mag. Concr. Res. 75 (19), 973–983.
Zhou, C.H., Chen, Z.P., 2017. Mechanical properties of recycled concrete made with different types of coarse aggregate. Construct. Build. Mater. 134, 497–506.
Zhou, F.P., Lydon, F.D., Barr, B.I.G., 1995. Effects of coarse aggregate on elastic modulus and compressive strength of high performance concrete. Cement Concr. Res. 25 (1), 177–186.